

# Analytical models for virus adsorption and inactivation in unsaturated porous media

Youn Sim, Constantinos V. Chrysikopoulos \*

*Department of Civil and Environmental Engineering, University of California, Irvine, CA 92697, USA*

Received 10 March 1998; accepted 16 February 1999

---

## Abstract

Analytical models for virus adsorption and inactivation in batch systems of homogeneous, isothermal, unsaturated porous media were developed. The models account for virus sorption onto liquid–solid as well as air–liquid interfaces and inactivation of viruses in the liquid phase and at both interfaces. Mathematical expressions appropriate for virus sorption onto liquid–solid and air–liquid interfaces were developed as functions of the soil moisture variation. The models were solved analytically by Laplace transform procedures. The effects of soil moisture variation on virus sorption at the liquid–solid as well as air–liquid interfaces were investigated. Available experimental data from virus adsorption-inactivation batch studies were successfully simulated by one of the models developed in this work. © 1999 Elsevier Science B.V. All rights reserved.

*Keywords:* Virus adsorption; Virus inactivation; Mathematical modeling; Analytical solution; Unsaturated porous media

---

## 1. Introduction

Virus survival and fate in unsaturated porous media are distinguished from those in saturated porous media, because virus adsorption and inactivation are considerably influenced by soil moisture variation and subsurface temperature fluctuation [6,22,23]. Unsaturated porous media consist of three phases: liquid; solid; and air phases. For water-wet solid surfaces, these three phases lead to liquid–solid and air–liquid interfaces [24]. Virus sorption within unsaturated porous media is signifi-

cantly controlled by the presence of these two interfaces. An illustration of the three phases present in unsaturated porous media, together with viruses in the liquid phase and at the associated two interfaces is shown in Fig. 1.

Virus sorption onto liquid–solid interfaces mainly results from electrostatic double-layer interactions and van der Waals forces [19]. Attachment of liquid phase viruses onto liquid solid interfaces is often described by a nonequilibrium kinetic relationship [22]. This adsorption process represents the rate of approach to equilibrium between adsorbed and liquid phase virus concentrations, by accounting for virus transport to the outer layer of a solid particle by mass transfer followed by virus immobilization.

---

\* Corresponding author. Tel.: +1-949-8248661; fax: +1-949-8243672.

*E-mail address:* costas@eng.uci.edu (C.V. Chrysikopoulos)

Recent investigations suggest that virus sorption is strongly correlated with the degree of soil moisture. Powelson et al. [13,14] and Poletika et al. [12] indicated that the enhanced removal of viruses at low soil moisture content is due to sorption of viruses onto air–liquid interfaces in addition to virus sorption onto liquid–solid interfaces and the degree of virus sorption at air–liquid interfaces is controlled by the level of soil moisture. Wan and Wilson [25] also demonstrated that colloids such as viruses strongly adsorb onto air–liquid interfaces. Powelson et al. [13] suggested that virus sorption is greater at air–liquid interfaces than liquid–solid interfaces, causing substantial reduction of liquid phase viruses.

Virus sorption at the air–liquid interface is essentially irreversible due to the strong binding of capillary forces. Because virus adsorption onto air–liquid interfaces in unsaturated porous media is influenced by fluctuations of the soil moisture content, the nonlinear relationship between soil moisture variation and virus adsorption onto air–liquid interfaces should be understood. An empirical approximation for virus sorption onto an air–liquid interface was presented by Thompson et al. [20]. However, quantitative relationships between soil moisture variation and virus adsorption are not available yet in the literature.

The inactivation of viruses is often considered as a first-order irreversible sink mechanism, with a rate constant accounting for all factors influencing virus inactivation [17,18,26]. The inactivation rate is smaller for viruses attached at a liquid–solid interface than viruses suspended in the liquid phase [5,8,22,26]. Thus, the inactivation rates for viruses in different phases should not be assumed equal [2,16,17].

There are several studies available in the literature focusing on virus adsorption and inactivation in batch systems of saturated porous media. For example, Vilker and Burge [23] developed a model for  $\phi$ x-174 phage adsorption in a batch system of saturated porous media, with negligible virus inactivation. Cookson and North [3] derived relatively simple kinetic models to simulate bacteriophage  $T_4$  adsorption onto activated carbon. Reddy et al. [15] developed empirical models for inactivation of microorganisms that incorpo-

rate the effects of temperature, soil moisture content, soil pH and adsorption of microorganisms onto the solid matrix. Hurst [9] employed linear and polynomial regression models to investigate the variation of virus inactivation rate coefficients associated with various external controlling factors. However, models accounting for virus adsorption and inactivation as a function of soil moisture variation in unsaturated porous media are not available in the literature.

The present study investigates the effect of soil moisture variation on virus adsorption and inactivation in unsaturated porous media. Appropriate mathematical models are developed and the corresponding analytical solutions are derived by Laplace transform techniques. However, the need for experimentally determined, quantitative relationships describing the mass transfer of virus particles to the liquid–solid and air–liquid interfaces as a function of moisture content, ionic strength and pH is not eliminated.

## 2. Model development

The adsorption and inactivation of viruses in a batch system of homogeneous, isothermal, unsaturated porous media are governed by the following expressions derived from mass balance considerations

$$\frac{d(\theta_m C)}{dt} = -k\theta_m[C - C_g] - k^\diamond\theta_m C - \lambda\theta_m C, \quad (1)$$

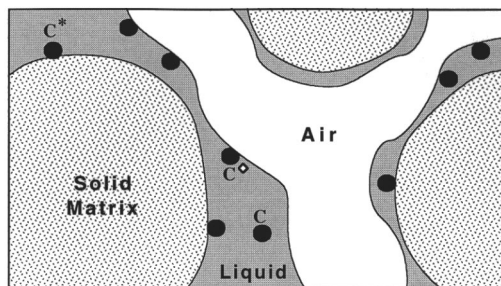


Fig. 1. Schematic illustration of viruses distributed in an unsaturated porous medium, where  $C$  represents viruses in the liquid phase,  $C^*$  viruses adsorbed at liquid–solid interface and  $C^\diamond$  viruses adsorbed at air–liquid interface.

$$\rho \frac{dC^*}{dt} = k\theta_m[C - C_g] - \lambda^* \rho C^*, \quad (2)$$

$$\frac{d(\theta_m C^\diamond)}{dt} = k^\diamond \theta_m C - \lambda^\diamond \theta_m C^\diamond, \quad (3)$$

$$\frac{d(\theta_m C_d)}{dt} = \lambda \theta_m C, \quad (4)$$

$$\rho \frac{dC_d^*}{dt} = \lambda^* \rho C^*, \quad (5)$$

$$\frac{d(\theta_m C_d^\diamond)}{dt} = \lambda^\diamond \theta_m C^\diamond, \quad (6)$$

where  $C$  is the liquid phase virus concentration;  $C_g$  is the liquid phase concentration of viruses in direct contact with solids;  $C^*$  is the adsorbed virus concentration at the liquid–solid interface;  $C^\diamond$  is the adsorbed virus concentration at the air–liquid interface; subscript  $d$  represents inactivated virus concentrations;  $k$  and  $k^\diamond$  are the liquid to liquid–solid and liquid to air–liquid interface mass transfer rates, respectively, representing the diffusive transport of viruses from the bulk solution to the respective interfaces;  $\theta_m$  is the soil moisture content; and  $\lambda$ ,  $\lambda^*$  and  $\lambda^\diamond$  are the inactivation rate coefficients of liquid phase viruses, adsorbed viruses at the liquid–solid interface and those at the air–liquid interface, respectively; and  $\rho$  is the bulk density of the solid matrix. Eq. (1) represents the rate of change of virus concentration in the liquid phase caused by virus sorption onto liquid–solid and air–liquid interfaces, as well as virus inactivation. The temporal change of virus concentration on the liquid solid and on air–liquid interfaces are described by Eqs. (2) and (3), respectively. Eqs. (4)–(6) represent the rate of change of inactivated virus concentrations in the liquid phase, liquid–solid and air–liquid interfaces, respectively. It is assumed that the following linear equilibrium relationship is valid [17]

$$C^*(t) = K_d C_g(t), \quad (7)$$

where  $K_d$  is the partition or distribution coefficient. Furthermore, the liquid to liquid–solid interface mass transfer rate is expressed as

$$k = \kappa a_T, \quad (8)$$

where  $\kappa$  is the liquid to liquid–solid interface mass transfer coefficient; and  $a_T$  is the specific liquid–solid interface area. The specific liquid–solid interface area is defined as the ratio of total surface area of the soil particles to the bulk volume of the porous medium [4]

$$a_T = \frac{3(1 - \theta)}{r_p}, \quad (9)$$

where  $r_p$  represents the average radius of soil particles and  $\theta$  is the porosity. Similarly, the liquid to air–liquid interface mass transfer rate is defined as

$$k^\diamond = \kappa^\diamond a_T^\diamond, \quad (10)$$

where  $\kappa^\diamond$  is the liquid to air–liquid interface mass transfer coefficient; and  $a_T^\diamond$  is the specific air–liquid interface area, defined as the ratio of the total air–liquid interface area to the bulk volume of the porous medium [1]

$$a_T^\diamond(\theta_m) = \frac{2\theta^b}{r_0} \left[ \zeta \theta_{m_r} \frac{\theta^{-b} - \theta_m^{-b}}{-b} + \frac{\theta^{1-b} - \theta_m^{1-b}}{1-b} \right], \quad (11)$$

where  $\zeta$  and  $b$  are empirical constants soil type specific;  $\theta_{m_r}$  is the residual or monolayer moisture content; and  $r_0$  is the effective pore radius at air entry which can be evaluated by the classical capillary rise equation with zero contact angle as follows [7]

$$r_0 = \frac{2\sigma}{\rho_w g h_0}, \quad (12)$$

where  $\sigma$  is the surface tension of water;  $\rho_w$  is the density of water;  $g$  is the gravitational constant; and  $h_0$  is the air-entry value, defined as the pore water head where air begins to enter water-saturated pores [7]. It should be noted that  $a_T^\diamond$  is a function of soil moisture content and takes a zero value when  $\theta_m = \theta$ . Thus, Eqs. (10) and (11) suggest that the liquid to air–liquid mass transfer rate,  $k^\diamond$ , decreases with increasing moisture content. Consequently, the virus mass transfer at the air–liquid interface is controlled by the soil moisture content. Fig. 2 illustrates the variation of the specific air–liquid interface area,  $a_T^\diamond$  and the corresponding mass transfer rates with soil moisture content for three soils, as evaluated by Eqs. (10)–

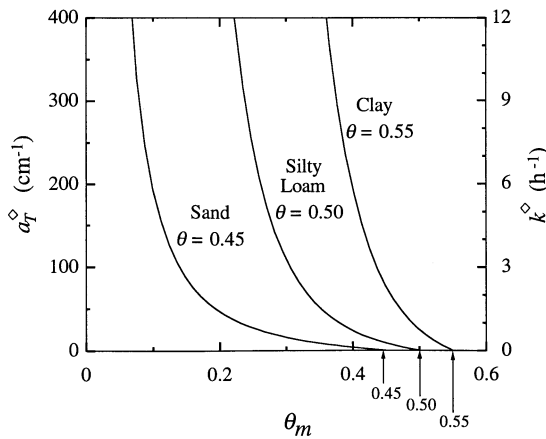


Fig. 2. Specific air–liquid interface area,  $a_T^\diamond$  and liquid to air–liquid interface mass transfer rate,  $k^\diamond$ , as a function of soil moisture content for three soil types ( $\kappa^\diamond = 0.03 \text{ cm h}^{-1}$ ). The empirical constants  $\zeta$ ,  $b$ ,  $h_0$  and  $\theta_{m_r}$  for different soil types were adopted from Cary [1] (for sand  $\zeta = 160$ ,  $b = 2$ ,  $h_0 = 2 \text{ cm}$ ,  $\theta_{m_r} = 0.0037$ ; for silt loam  $\zeta = -0.614$ ,  $b = 5$ ,  $h_0 = 10 \text{ cm}$ ,  $\theta_{m_r} = 0.0310$ ; for clay  $\zeta = -0.908$ ,  $b = 7.5$ ,  $h_0 = 30 \text{ cm}$ ,  $\theta_{m_r} = 0.0775$ ).

(12). The three soil types examined are: sand; silty loam; and clay. The empirical constants associated with Eq. (11) were obtained from Cary [1] and they are listed in Table 1. It is shown that both  $a_T^\diamond$  and  $k^\diamond$  take a zero value when the soils are completely saturated ( $\theta_m = \theta$ ) and drastically increase as the soil moisture decreases.

The appropriate initial conditions for the batch system are given by

Table 1  
Model parameters for simulations

Parameter	Value	Reference
$b$	2	Cary [1]
$g$	$980 \text{ cm s}^{-2}$	–
$h_0$	2 cm	Cary [1]
$K_d$	$20 \text{ cm}^3 \text{ g}^{-1}$	Vilker and Burge [23]
$r_p$	0.1 cm	Vilker and Burge [23]
$\zeta$	160	Cary [1]
$\theta$	0.45	Cary [1]
$\theta_{m_r}$	0.0037	Cary [1]
$\kappa$	$0.006 \text{ cm h}^{-1}$	Vilker and Burge [23]
$\rho$	$1.5 \text{ g cm}^{-3}$	Yates and Ouyang [27]
$\rho_w$	$1 \text{ g cm}^{-3}$	Guymon [7]
$\sigma$	$0.0742 \text{ N m}^{-1}$	Guymon [7]

$$C(0) = C_i, \quad (13a)$$

$$C^*(0) = 0, \quad (13b)$$

$$C^\diamond(0) = 0, \quad (13c)$$

$$C_d(0) = 0, \quad (14a)$$

$$C_d^*(0) = 0, \quad (14b)$$

$$C_d^\diamond(0) = 0, \quad (14c)$$

where  $C_i$  is the initial liquid phase virus concentration.

For a batch system with fixed moisture content (constant  $\theta_m$ ), the governing Eqs. (1)–(6) subject to conditions Eqs. (13a), (13b), (13c), (14a), (14b) and (14c) are solved by employing Laplace transform techniques. The desired analytical solutions are:

$$C(t) = C_i \left[ \frac{(\Phi - m_1)e^{-m_1 t} - (\Phi - m_2)e^{-m_2 t}}{m_2 - m_1} \right], \quad (15)$$

$$C^*(t) = \frac{C_i \theta_m k}{\rho} \left[ \frac{e^{-m_1 t} - e^{-m_2 t}}{m_2 - m_1} \right], \quad (16)$$

$$\begin{aligned} C^\diamond(t) &= \left( \frac{C_i k^\diamond}{\lambda^\diamond - \lambda^\diamond d_1 + d_2} \right) \\ &\times \left\{ (\Phi - \lambda^\diamond) \exp[-\lambda^\diamond t] \right. \\ &+ (\lambda^\diamond - \Phi) \left[ \frac{m_2 e^{-m_2 t} - m_1 e^{-m_1 t}}{m_2 - m_1} \right] \\ &+ (\Phi \lambda^\diamond - \Phi d_1 + d_2) \left[ \frac{e^{-m_1 t} - e^{-m_2 t}}{m_2 - m_1} \right] \left. \right\}, \quad (17) \end{aligned}$$

$$\begin{aligned} C_d(t) &= C_i \lambda \left\{ \frac{\Phi}{d_2} - \frac{\Phi}{d_2} \left[ \frac{m_2 e^{-m_2 t} - m_1 e^{-m_1 t}}{m_2 - m_1} \right] \right. \\ &+ \left. \left( 1 - \frac{\Phi d_1}{d_2} \right) \left[ \frac{e^{-m_1 t} - e^{-m_2 t}}{m_2 - m_1} \right] \right\}, \quad (18) \end{aligned}$$

$$\begin{aligned} C_d^*(t) &= \frac{C_i \lambda^* \theta_m k}{d_2 \rho} \left[ 1 - \left( \frac{d_1 - m_1}{m_2 - m_1} \right) e^{-m_1 t} \right. \\ &- \left. \left( \frac{m_2 - d_1}{m_2 - m_1} \right) e^{-m_2 t} \right], \quad (19) \end{aligned}$$

$$\begin{aligned}
 & C_d^\diamond(t) \\
 &= \left( \frac{C_i \lambda^\diamond k^\diamond}{\lambda^{\diamond 2} - \lambda^\diamond d_1 + d_2} \right) \\
 &\quad \times \left\{ \left( \frac{\Phi}{\lambda^\diamond} - 1 \right) (1 - \exp[-\lambda^\diamond t]) \right. \\
 &\quad + (\lambda^\diamond - \Phi) \left[ \frac{e^{-m_1 t} - e^{-m_2 t}}{m_2 - m_1} \right] \\
 &\quad + \left( \frac{\Phi \lambda^\diamond}{d_2} - \frac{\Phi d_1}{d_2} + 1 \right) \\
 &\quad \left. \times \left[ 1 - \left( \frac{d_1 - m_1}{m_2 - m_1} \right) e^{-m_1 t} - \left( \frac{m_2 - d_1}{m_2 - m_1} \right) e^{-m_2 t} \right] \right\}, \quad (20)
 \end{aligned}$$

where

$$\Phi = \frac{k \theta_m}{\rho K_d} + \lambda^*, \quad (21)$$

$$m_1 = \frac{1}{2} [d_1 - (d_1^2 - 4d_2)^{1/2}], \quad (22)$$

$$m_2 = \frac{1}{2} [d_1 + (d_1^2 - 4d_2)^{1/2}], \quad (23)$$

$$d_1 = \Phi + k + \lambda + k^\diamond, \quad (24)$$

$$d_2 = \Phi(k + \lambda + k^\diamond) - \frac{k^2 \theta_m}{\rho K_d}. \quad (25)$$

It should be noted that the following relationship is always valid at any time  $t$  so that the total virus mass (infective or live viruses plus inactivated or dead viruses) in the batch system is conserved

$$C + \frac{\rho}{\theta_m} C^* + C^\diamond + C_d + \frac{\rho}{\theta_m} C_d^* + C_d^\diamond = C_i. \quad (26)$$

For the special case where the inactivation of viruses is ignored ( $\lambda = \lambda^* = \lambda^\diamond = 0$ ) in saturated porous media ( $\theta_m = \theta$ ), Eq. (15) reduces to the analytical solution presented by Vermeulen and Hiester [21].

### 3. Model simulations and discussion

In order to illustrate the effect of soil moisture variations on virus deposition and removal in

unsaturated porous media, model simulations are performed for a variety of situations. Because values for  $\kappa^\diamond$  are not available in the literature, it is assumed that  $\kappa^\diamond = 5\kappa$ . This assumption is based on the experimental observations that colloid particles are more strongly sorbed onto the air–liquid interface than onto the liquid–solid interface [25]. Unless specified otherwise, all the fixed model parameter values used for model simulations are listed in Table 1. The values for empirical constants  $\zeta$ ,  $b$ ,  $h_0$  and  $\theta_m$  measured for sand are adopted from Cary [1]. All virus concentrations are conveniently normalized by the initial concentration. As suggested by Yates and Ouyang [27], the inactivation rate coefficients of viruses adsorbed onto a liquid–solid interface are approximately one half of the coefficients for liquid phase viruses ( $\lambda^* = \lambda/2$ ) owing to the protective effect of the solid matrix. Furthermore, because there is no quantitative relationship between  $\lambda$  and  $\lambda^\diamond$  available in the literature, in this study we assume that  $\lambda^\diamond = \lambda$ .

Fig. 3 illustrates the time dependence of the various virus concentrations within the batch unsaturated system considered in this work. The normalized concentration profiles of infective and inactivated viruses are presented separately in Fig. 3(a,b), respectively. In Fig. 3(a), the rapid decrease of the liquid phase virus concentration is attributed to the fast increase of irreversible virus sorption onto air–liquid interfaces and to the relatively gradual increase of virus sorption onto liquid–solid interfaces. It should be noted, however, that due to virus inactivation both  $C^*$  and  $C^\diamond$  also vanish at large time. It is shown in Fig. 3(b) that most of the virus inactivation occurs at the air–liquid interface, because for the particular soil moisture content employed here ( $\theta_m = 0.25$ ), as shown in Fig. 3(a), the majority of the liquid phase viruses are adsorbed at the air–liquid interface and subsequently undergo inactivation. It should be noted, however, that eventually the inactivated virus concentrations in the liquid phase and at liquid–solid and air–liquid interfaces reach their asymptotic values (0.099, 0.092, 0.8, respectively) because most of the liquid phase viruses initially present in the batch system are inactivated either in the liquid phase or at the interfaces.

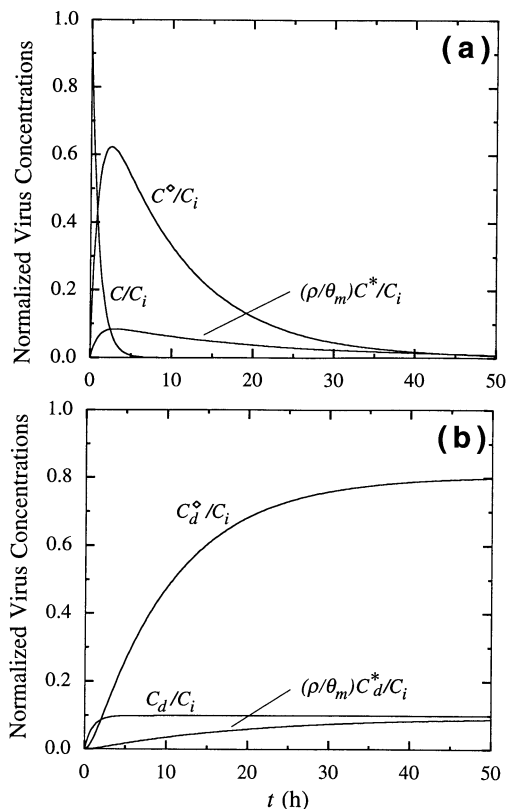


Fig. 3. Normalized concentration profiles of (a) infective and (b) inactivated viruses as a function of time ( $\lambda = 0.1 \text{ h}^{-1}$ ,  $\lambda^* = \lambda/2$ ,  $\lambda^{\diamond} = \lambda$ ,  $\kappa^{\diamond} = 5\kappa$  and  $\theta_m = 0.25$ ).

In order to investigate the effect of virus adsorption at the liquid–solid interface on the total infective virus concentration within a saturated porous medium,  $[C + (\rho/\theta_m)C^*]/C_i$  as a function of increasing liquid to liquid–solid interface mass transfer rate,  $k$ , is plotted in Fig. 4. Saturated conditions have been selected so that the sorption at air–liquid interface is neglected ( $a_T^{\diamond} = 0$ ,  $k^{\diamond} = 0$ ). It is evident from Fig. 4 that increasing virus sorption onto the liquid–solid interface, more viruses survive either in the liquid phase or adsorbed at the liquid–solid interface. This is an intuitive result because the virus inactivation rate at the liquid–solid interface is assumed smaller than the liquid phase inactivation rate ( $\lambda^* = \lambda/2$ ). This result explains that viruses survive for a longer period of time in a porous medium which accommodates more virus sorption onto liquid–

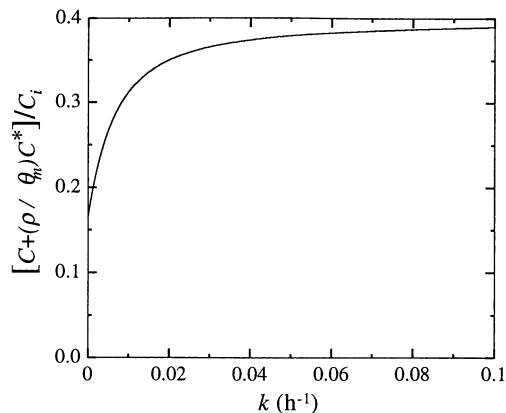


Fig. 4. Effect of the liquid to liquid–solid interface mass transfer rate,  $k$ , on the normalized total concentration of infective viruses in a saturated system ( $t = 18 \text{ h}$ ,  $\lambda = 0.1 \text{ h}^{-1}$ ,  $\lambda^* = \lambda/2$  and  $\theta_m = \theta$ ).

solid interfaces. Such a porous medium should have a large specific liquid–solid interface area ( $a_T$ ) because the virus mass transfer onto a liquid–solid interface is directly proportional to  $a_T$  (see Eq. (8)).

The effect of soil moisture content on virus concentrations in the liquid phase, onto the liquid–solid and air–liquid interfaces are illustrated in Fig. 5 for the special case where virus inactivation throughout the system considered here is

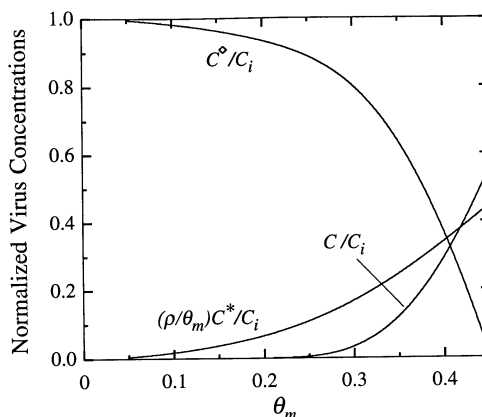


Fig. 5. Effect of the soil moisture content on the normalized virus concentration in the liquid phase,  $C/C_i$ , adsorbed at liquid solid interface,  $(\rho/\theta_m)C^*/C_i$  and adsorbed at the air–liquid interface,  $C^{\diamond}/C_i$  ( $t = 6 \text{ h}$ ,  $\lambda = \lambda^* = \lambda^{\diamond} = 0$  and  $\kappa^{\diamond} = 5\kappa$ ).

Table 2  
Parameters associated with the *Poliovirus-1* batch experiment

<i>Experimental parameters</i> [8]	
$r_p$	0.05 cm (average)
$\theta$	0.45
$\rho$	1.55 g cm <sup>-3</sup>
<i>Estimated parameters</i>	
$k$	0.00439 h <sup>-1</sup>
$K_d$	0.0865 cm <sup>3</sup> g <sup>-1</sup>
$k^\diamond$	0.00124 h <sup>-1</sup>
sse	0.434
<i>Calculated parameters</i>	
$a_T$	33 cm <sup>-1</sup>
$a_T^\diamond$	86.34 cm <sup>-1</sup>
$\kappa$	0.000133 cm h <sup>-1</sup>
$\kappa^\diamond$	0.0000143 cm h <sup>-1</sup>

assumed negligible ( $\lambda = \lambda^* = \lambda^\diamond = 0$ ). As soil moisture content decreases, the normalized virus concentration at the air–liquid interface rapidly increases, whereas the virus concentrations in the liquid phase and at the liquid solid interface vanish rapidly. This is because at low soil moisture content the majority of liquid phase viruses are adsorbed onto the air–liquid interface and only a small amount of viruses are left in suspension or adsorbed onto the liquid–solid interface. However, increasing the soil moisture close to soil saturation ( $\theta_m = \theta = 0.45$ ) leads to increasing virus concentrations in the liquid phase and at the liquid–solid interface because more viruses in the liquid phase are in contact with the liquid–solid interface. In contrast, increasing the soil moisture results in decreasing the air–liquid interface area and consequently, in reducing virus sorption onto the air–liquid interface.

The analytical expression derived for liquid phase virus concentration Eq. (15) is employed to simulate data from *Poliovirus-1* adsorption-inactivation experiment in a loamy sand batch system reported by Hurst et al. [8]. The experiment was conducted in a batch system partially saturated with sewage effluent at 15% soil moisture content under sterile conditions. Since the experiment was conducted at a very low temperature (1°C), for simplicity it is assumed that  $\lambda = \lambda^* = \lambda^\diamond = 0$ . Given the experimental parameters listed in Table 2, the values for  $k$ ,  $K_d$  and  $k^\diamond$  are estimated by a

nonlinear least squares regression method [10,11]. The parameter  $\kappa$  was calculated by Eq. (8) with a value for  $a_T$  estimated by Eq. (9). Similarly, the parameter  $\kappa^\diamond$  was calculated from the estimated value of  $k^\diamond$  by employing Eq. (10) with  $a_T^\diamond$  as estimated by Eq. (11) with necessary values for  $\theta_m$ ,  $\zeta$ ,  $b$  and  $h_0$  obtained from the work by Cary [1], assuming that the average size of the soil material in the batch system is similar to sand with  $r_p \approx 0.05$  cm and  $\theta = 0.45$  [1,7]. The estimated and calculated parameter values together with the corresponding residual sums of squared error (sse) are presented in Table 2. Fig. 6 clearly shows a relatively good agreement between the simulated concentration history (solid line) and the *Poliovirus-1* experimental data (circles).

#### 4. Summary

Analytical models applicable to virus adsorption and inactivation in batch systems of homogeneous, isothermal unsaturated porous media were developed, accounting for soil moisture controlled virus adsorption onto the liquid–solid as well as air–liquid interfaces and virus inactivation in the liquid phase and at the interfaces. The analytical expressions for both infective and inactivated virus concentrations in the liquid phase and at both interfaces were presented. Model simulations indicated that viruses may survive for a longer period of time within a porous medium with large

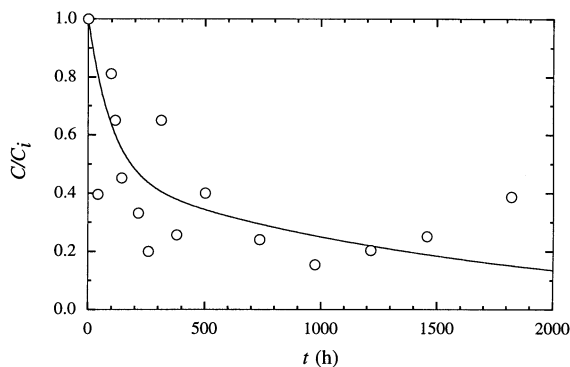


Fig. 6. Normalized concentrations of *Poliovirus-1* data (circles) adopted from Hurst et al. [8] and simulated concentration history (solid curve).

specific liquid–solid interface area which accommodates more virus sorption onto the liquid–solid interface. It was shown that virus survival in unsaturated porous media is highly sensitive to soil moisture variation. At low soil moisture, virus removal is significantly enhanced due to the irreversible adsorption of viruses onto the air–liquid interface. The analytical expression for the liquid phase virus concentration fitted successfully existing experimental data. The analytical expressions presented in this study can effectively be utilized in verifying the results from batch experiments examining the effect of soil moisture on the adsorption and inactivation of viruses in unsaturated porous media.

## 5. Notation

$a_T$	specific liquid solid interface area, $L^2/L^3$
$a_T^\diamond$	specific air–liquid interface area, $L^2/L^3$
$b$	empirical constant
$C$	concentration of viruses in suspension (liquid phase), $M/L^3$
$C^*$	deposited virus concentration at the liquid solid interface (virus mass/solids mass), $M/M$
$C^\diamond$	adsorbed virus concentration at the air–liquid interface, $M/L^3$
$C_g$	concentration of viruses directly in contact with solids, $M/L^3$
$C_i$	initial liquid phase virus concentration, $M/L^3$
$d_1$	defined in Eq. (24)
$d_2$	defined in Eq. (25)
$g$	gravitational constant, $L/t^2$
$h_0$	air-entry value, $L$
$k$	liquid to liquid–solid interface mass transfer rate, $t^{-1}$
$k^\diamond$	liquid to air–liquid interface mass transfer rate, $t^{-1}$
$K_d$	partition or distribution coefficient, $L^3/M$
$m_1$	defined in Eq. (22)
$m_2$	defined in Eq. (23)
$r_0$	effective pore radius at air-entry, $L$
$r_p$	average radius of soil particles, $L$
$t$	time, $t$

## Greek letters

$\beta$	empirical constant
$\zeta$	empirical constant
$\theta$	porosity (void volume/porous medium volume), $L^3/L^3$
$\theta_m$	soil moisture content (liquid volume/porous medium volume), $L^3/L^3$
$\theta_{m_r}$	residual or monolayer moisture content (liquid volume/porous medium volume), $L^3/L^3$
$\kappa$	liquid to liquid–solid interface mass transfer coefficient, $L/t$
$\kappa^\diamond$	liquid to air–liquid interface mass transfer coefficient, $L/t$
$\lambda$	inactivation rate coefficient of liquid phase viruses, $t^{-1}$
$\lambda^*$	inactivation rate coefficient of adsorbed viruses at the liquid–solid interface, $t^{-1}$
$\lambda^\diamond$	inactivation rate coefficient of adsorbed viruses at the air–liquid interface
$\rho$	bulk density of the solid matrix (solids mass/aquifer volume), $M/L^3$
$\rho_w$	water density, $M/L^3$
$\Phi$	defined in Eq. (21)
$\sigma$	surface tension of water, $M/t^2$

## Subscripts

$d$	concentration of inactivated viruses
$i$	initial concentration

## Acknowledgements

This work was sponsored by the National Water Research Institute and the University of California Water Resources Center, as part of Water Resources Center Project W-890. The content of this manuscript does not necessarily reflect the views of the Agencies and no official endorsement should be inferred.

## References

- [1] J.W. Cary, J. Contam. Hydrol. 15 (1994) 243.
- [2] C.V. Chrysikopoulos, Y. Sim, J. Hydrol. 185 (1996) 199.
- [3] J.T. Cookson Jr., W.J. North, Env. Sci. Tech. 1 (1967) 46.

- [4] H.S. Fogler, *Elements of Chemical Reaction Engineering*, 2, Prentice Hall, Englewood Cliffs, NJ, 1992.
- [5] C.P. Gerba, *Adv. Appl. Microb.* 30 (1984) 133.
- [6] C.P. Gerba, M.V. Yates, S.R. Yates, Quantitation of factors controlling viral and bacterial transport in subsurface, in: C.J. Hurst (Ed.), *Modeling the Environmental Fate of Microorganisms*, American Society for Microbiology, Washington, DC, 1991.
- [7] G.L. Guymon, *Unsaturated Zone Hydrology*, Prentice Hall, Englewood Cliffs, NJ, 1994.
- [8] C.J. Hurst, C.P. Gerba, I. Cech, *Appl. Environ. Microb.* 40 (1980) 1067.
- [9] C.J. Hurst, Using linear and polynomial models to examine the environmental stability of viruses, in: C.J. Hurst (Ed.), *Modeling the Environmental Fate of Microorganisms*, American Society for Microbiology, Washington, DC, 1991.
- [10] IMSL MATH/LIBRARY User's Manual, ver. 2.0. IMSL, Houston TX, 1991.
- [11] D. Kahaner, C. Moler, S. Nash, *Numerical Methods and Software*, Prentice Hall, Englewood Cliffs, NJ, 1989.
- [12] N.N. Poletika, W.A. Jury, M.V. Yates, *Water Resour. Res.* 31 (1995) 801.
- [13] D.K. Powelson, J.R. Simpson, C.P. Gerba, *J. Environ. Qual.* 19 (1990) 396.
- [14] D.K. Powelson, J.R. Simpson, C.P. Gerba, *Appl. Environ. Microb.* 57 (1991) 2192.
- [15] K.R. Reddy, R. Khaleel, M.R. Overcash, *J. Environ. Qual.* 10 (1981) 255.
- [16] Y. Sim, C.V. Chrysikopoulos, *Water Resour. Res.* 31 (1995) 1429.
- [17] Y. Sim, C.V. Chrysikopoulos, *Water Resour. Res.* 32 (1996) 2607.
- [18] Y. Sim, C.V. Chrysikopoulos, *Transport Porous Media* 30 (1998) 87.
- [19] G. Teutsch, K. Herbold-Paschke, D. Tougianidou, T. Hahn, K. Botzenhart, *Water Sci. Tech.* 24 (1991) 309.
- [20] S.S. Thompson, M. Flury, M.V. Yates, *Appl. Environ. Microb.* 64 (1998) 304.
- [21] T. Vermeulen, N.K. Hiester, Adsorption and ion exchange, in: R.H. Perry, C.H. Chilton (Eds.), *Chemical Engineers Handbook*, 5, McGraw-Hill, New York, 1973.
- [22] V.L. Vilker, Simulating virus movement in soils, in: I.K. Iskandar (Ed.), *Modeling Waste Renovation: Land Treatment*, Wiley, New York, 1981, pp. 223–253.
- [23] V.L. Vilker, W.D. Burge, *Water Res.* 14 (1980) 783.
- [24] J. Wan, J.L. Wilson, New findings on particle transport within the vadose zone; the role of the gas–water interface, in: H.J. Morel-Seytoux (Ed.), *Twelfth Annual American Geophysical Union Hydrology Days*, Fort Collins CO, 1992, pp. 402–419.
- [25] J. Wan, J.L. Wilson, *Water Resour. Res.* 30 (1994) 11.
- [26] M.V. Yates, S.R. Yates, *Crit. Rev. Environ. Control.* 17 (1988) 307.
- [27] M.V. Yates, Y. Ouyang, *Appl. Environ. Microb.* 58 (1992) 1609.